An unexpectedly large working stroke from chymotryptic fragments of myosin II

J.E. Molloy[a], J. Kendrick-Jones[b], C. Veigel[a], R.T. Tregear[b,*]

[a] *Department of Biology, University of York, York Y01 5DW, UK*
[b] *MRC Laboratory of Molecular Biology, Hills Road, Cambridge CB2 2QH, UK*

Received 16 June 2000; revised 2 August 2000; accepted 2 August 2000

Edited by Matti Saraste

Abstract Recent structural evidence indicates that the light chain domain of the myosin head (LCD) bends on the motor domain (MD) to move actin. Structural models usually assume that the actin-MD interface remains static and the possibility that part of the myosin working stroke might be produced by rotation about the acto-myosin interface has been neglected. We have used an optical trap to measure the movement produced by proteolytically shortened single rabbit skeletal muscle myosin heads (S-1(A1) and S-1(A2)). The working stroke produced by these shortened heads was more than that which the MD-LCD bend mechanism predicts from the full-length (papain) S-1's working stroke obtained under similar conditions. This result indicates that part of the working stroke may be caused by motor action at the actin-MD interface.

Key words: Myosin; Working stroke; Optical trap; Motor; Muscle; Single molecule

1. Introduction

The mechanism by which myosin generates motion remains debatable. On the one hand, there are several lines of evidence showing that myosin II generates motion by bending internally at the junction between its motor domain (MD) and its light chain domain (LCD). Crystal structures of the myosin II head with different nucleotide analogues bound at its enzymatic site show structural alterations in the adjacent converter region, leading to a set of different angles of the MD-LCD bend [1]. Cryo-electron microscopy of myosin II heads bound to actin filaments reveals a change in the MD-LCD angle between the ADP-bound state and nucleotide-free (rigor) state [2] while rapid freezing of active muscle shows a variety of MD-LCD angles in myosin heads attached to actin [3]. Furthermore, electron paramagnetic resonance of myosin II heads on thick filaments shows that the MD rotates relative to the LCD [4]. Other measurements are equivocal. Both fluorescence polarisation and X-ray diffraction measurements show that the LCD rotates during stretch or release of active muscle [5,6] but do not, as yet, determine whether the MD rotates as well.

On the other hand, there is evidence that bending may occur at the actin-MD attachment interface. Both *Dictyostelium* myosin II MD constructed without light chains [7,8] and proteolytically derived skeletal muscle MD without light chains [9] move actin in vitro. Cryo-electron microscopy of active myosin II molecules shows a range of MD attachment angles to actin [10,11] and in smash-frozen active insect flight muscle those myosin heads that contact actin in an anti-rigor manner do so at a different angle to those that present in a rigor-like manner [3]. Finally myosin XIV, which has the enzymatic characteristics of a motor protein [12] and is presumed to be a motor, has no LCD and could scarcely act by an MD-LCD bend.

On either of the proposed mechanisms the LCD acts as a lever arm, so that a decrease of its length should produce a reduction both of unloaded actin velocity in the classic motility assay, and of working stroke in single-molecule interaction experiments. The difference between the predictions of the mechanisms lies in the magnitude of the expected effect. Several techniques have been used to alter the length of the LCD; the structure of the natural LCD of skeletal myosin II has been reduced [9], while the LCD on *Dictyostelium* myosin II has been changed in length [8] or replaced by actinin repeats [13,14]. A linearity between actin velocity and LCD length intercepting the axis close to the expected MD-LCD fulcrum was obtained from *Dictyostelium* constructs [8]. This strongly supported the MD-LCD bend hypothesis; the authors pointed out, however, that it did not exclude some rotation at the actin-MD interface. A recent preliminary report of single molecule displacements at low load from *Dictyostelium* myosin II constructs [14] also supports the MD-LCD bend hypothesis.

The present experiments were conducted in order to further test the point. Three recent optical trap studies [15–17] and one scanning probe study [18] on skeletal muscle myosin II heads have reported motor strokes of 5–6 nm, providing an accepted baseline to work from. We shortened the LCD domain of rabbit skeletal muscle myosin II by proteolytic removal of the regulatory light chain binding domain and observed the working stroke in an optical trap; it was greater than that predicted by the MD-LCD bend hypothesis.

2. Materials and methods

2.1. Protein preparation

Skeletal rabbit myosin was prepared by classical procedures [19] and stored in 0.6 M NaCl, 25 mM phosphate pH 7.5, 5 mM dithio-

*Corresponding author. Fax: (44)-1223-213556.
E-mail: rt1@mrc-lmb.cam.ac.uk

Abbreviations: MD, motor domain; LCD, light chain binding domain; S-1, subfragment 1, the digestion product containing the motor head of myosin; S-1(A1), S-1(A2), the chymotryptically derived motor head isoenzymes; ELC, essential light chain; RLC, regulatory light chain

0014-5793/00/$20.00
PII: S0014-5793(00)01937-2

threitol (DTT) and 50% glycerol at −20°C. Subfragment 1 (S-1) was prepared as in [20]. The myosin (50 ml at 15 mg/ml in the 50% glycerol solution) was dialysed overnight against two changes of 2 l of 20 mM NaCl, 10 mM phosphate pH 6.8, 0.2 mM DTT. The precipitated myosin was washed once to remove the remaining glycerol and resuspended with gentle homogenisation in 125 mM NaCl, 25 mM phosphate pH 7.2, 1 mM EDTA, 1 mM DTT at a concentration of 15 mg/ml. After equilibration at 20°C it was digested with α-chymotrypsin (Sigma C-3142 TLCK-treated) at a protein:enzyme weight ratio of 300:1 for 8 min. Digestion was stopped by the addition of 100 mM phenylmethylsulphonyl fluoride slowly to a final concentration of 0.5 mM. The digest was dialysed against 2 l of 50 mM imidazole pH 6.8, 1 mM DTT for 2 h and chromatographed on a DEAE-cellulose column (Whatman DE-52 [20]). The resultant isoenzymes of regulatory light chain (RLC)-free S-1 (S-1(A1) and S-1(A2)) were separated by this ion exchange chromatography step and were pooled, concentrated by Amicon ultrafiltration and stored in 20% sucrose, 100 mM NaCl, 50 mM imidazole pH 6.8, 5 mM DTT (at 20 mg/ml) at −80°C. G-actin was prepared by classical methods [20] and stored at −80°C. Rhodamine-phalloidin was purchased from Molecular Probes.

2.2. Assay components

G-actin was polymerised by addition of salt and magnesium and reacted at low concentration with rhodamine-phalloidin (molar ratio 2 phalloidin:1 actin monomer). S-1(A1) and S-1(A2) were cleared of unreactive molecules ('dead heads') by ultracentrifugation in the presence of MgATP and F-actin (molar ratio 4 S-1:1 actin). *N*-Ethylmaleimide-modified myosin-coated polystyrene beads for attachment of F-actin were prepared as previously described [16].

2.3. Experimental protocol

The dual optical trap and nitrocellulose-coated flow cell were as described [16,21]. In the present experiments, only a single four-quadrant detector was used. Laser power was adjusted to set the combined optical trap stiffness, K_{trap}, at 0.02–0.04 pN/nm, about 10–50 times lower than that of the acto-myosin cross-bridge. All experiments were performed at 23°C in a neutral, MgATP-containing and calcium-free solution of low ionic strength (25 mM KCl, 1 mM EGTA, 4 mM $MgCl_2$, ATP 3 μM, creatine phosphate (CP) 2 mM, creatine phosphokinase (CPK) 0.5 mg/ml, bovine serum albumin (BSA) 0.5 mg/ml, 25 mM imidazole buffer at pH 7.4). Photobleaching was inhibited by including an oxygen scavenger system (glucose 3 mg/ml, 0.05 mg/ml glucose oxidase, 0.02 mg/ml catalase, 20 mM DTT). During the optical trapping experiments the in vitro assay flow cell was sealed with grease to prevent water evaporation and diffusion of oxygen into the cell; accumulation of gluconic acid from the oxygen scavenger reaction would cause a drop in pH and precipitation of BSA. Inclusion of 2 mM CP/CPK ensured ATP concentration was maintained constant. At the start of each experimental series the system was tested by applying 100 μg/ml (as a 0.1 ml aliquot to a 480 mm^2 exposed area of nitrocellulose-coated coverslip) of S-1(A1) or S-1(A2) and 1 mM MgATP to a flow cell and the resultant actin motion checked for regularity and speed. In subsequent flow cells both the S-1 and ATP concentrations were lowered until acto- S-1 attachments of adequate length to observe, separated sufficiently to obviate overlap, were obtained (5 μg/ml protein, applied as before with 3 μM ATP).

The working lifetime of a given optically trapped actin filament was usually 1–2 h and was limited by breakage or contamination of one of the optically trapped beads by either a free bead or other debris wandering into the optical tweezer. Long sets of events were usually obtained from several different surface loci (and hence different S-1 molecules). The orientation of some actin filaments was occasionally reversed during their lifetime, in order to check for the reversal of the observed displacement orientation. The position detector (four-quadrant photodiode) and optical tweezer stiffness were calibrated for each bead tested.

2.4. Data analysis

Attachment between actin and S-1 was detected by the reduced longitudinal thermal vibration of the trapped bead–actin filament–bead dumbbell (Fig. 1; for experimental details see [16]). A running value of data variance was calculated and displayed (Fig. 1). The calculated local variance gives a measure of the immediate system stiffness (since $\kappa_{sys} = k_b T / \langle \text{variance} \rangle$, where $k_b T$ = thermal energy) and this changes dramatically when the myosin (bound to the coverslip, which acts as a mechanical ground) attaches to the actin filament. However, viscous drag on the 1 μm diameter beads causes the mechanical system to be over-damped. Brownian noise is therefore correlated in time and local estimates of variance are an unrobust measure of system stiffness; in the current analysis we therefore used a 15 ms running window to estimate the variance and then applied a running median filter (30 ms window size) to these data and set the cutoff level for the significance of the variance reduction due to myosin attachment at a stiffness equivalent to >0.1 pN/nm. We only accepted attachments >45 ms in duration. We calculated the amplitude of the displacement during the attachment relative to the local mean position measured for up to 1 s before and after the event. Duration of attachment intervals and time between adjacent attachment events was also recorded.

Displacements were assembled for each actin filament. Overall data were taken from 12 actin filaments; the average data set contained 218 events. Within each set, when the actin filament was reversed in orientation the sign of the mean displacement was reversed. The overall mean of each actin filament data set was made positive, by appropriate reversal of the entire set. Data were then pooled for each isoenzyme (S-1(A1) and S-1(A2)). The time courses of attachment and detachment were plotted and fitted to single exponential curves (amplitude and time constant fitted by Kaleidagraph iteration; cf. Fig. 2). The displacements for each isoenzyme were histogrammed using 5 nm interval bins (use of this bin size had very little effect on the calculated mean). The resultant histograms were fitted to Gaussian curves (mean, peak and width fitted by Kaleidagraph iteration; cf. Fig. 3). A histogram of the distribution of the free bead position in the absence of attachments was also plotted (not shown); this plot showed a similar distribution width (within 10%) to those of the experimental histograms. The standard deviations of both histograms were consistent with the combined optical tweezer stiffness being approx. 0.035 pN/nm.

3. Results

When either S-1(A1) or S-1(A2) was bound in the flow cell at high concentrations (100 μg/ml S-1 isoenzyme added as described in Section 2) actin filaments moved continuously over the myosin-coated surface. At intermediate concentration of protein (20 μg/ml), actin did not adhere to the surface, but an optically trapped actin filament adjacent to the surface was progressively displaced up to 100 nm before it detached. At a still lower protein concentration (2–10 μg/ml) the actin made contact without being progressively displaced. The duration of the non-progressive contacts rose as the ATP concentration was lowered, and their incidence decreased as the protein concentration was lowered. A convenient protocol for observation of discrete events was provided by 5 μg/ml added S-1

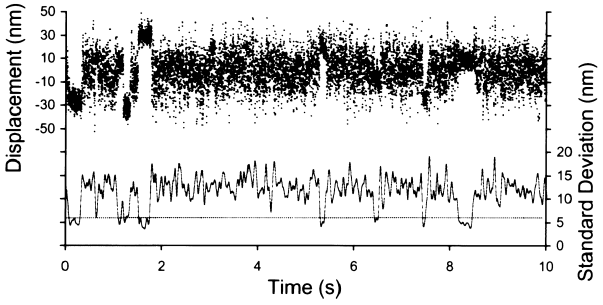

Fig. 1. Displacement of actin filament held under a low trap stiffness when an individual S-1(A1) molecule makes contact. Note the abrupt reduction in thermally generated longitudinal vibration of the actin filament–bead pair; this was used as a criterion of contact via the running estimate of variance (lower trace). Similar records were obtained from S-1(A2); data not shown. Assay conditions: 5 μg/ml S-1(A1); 3 μM MgATP; $K_{trap} = 0.035$ pN/nm; 23°C.

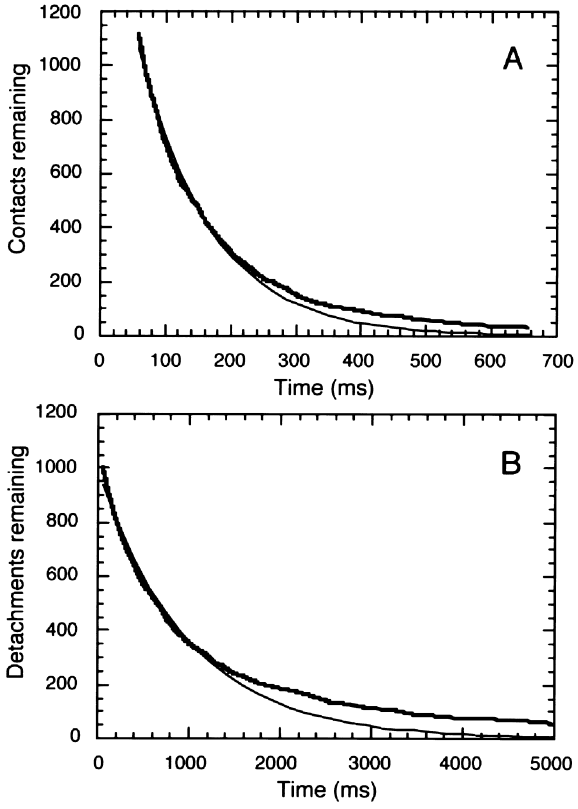

Fig. 2. Time course of detachment (A) and attachment (B) of S-1(A1). The thicker lines are the data, the thinner lines are fitted exponentials ($\tau_{det} = 111$ ms; $\tau_{att} = 980$ ms). Similar fits were obtained from S-1(A2) ($\tau_{det} = 101$ ms; $\tau_{att} = 1230$ ms; data not shown).

isoenzyme and 3 μM Mg ATP. Actin filament binding to either myosin isoenzyme greatly increased the stiffness of the trapped filament (Fig. 1). This allowed both the attachment duration and its displacement relative to the mean position of the trapped filament in the absence of contact to be accurately assessed.

The lifetime of S-1 attachment to actin followed an approximately exponential time course (Fig. 2A), indicating a first-order process. The fitted exponents for the two isoenzymes were similar (Fig. 2, legend). The detachment rate (governing the attached lifetime) was ATP-sensitive so the rate-limiting step was assumed to be ATP binding. On this basis, the apparent rate constant for ATP attachment was 3×10^6 M^{-1} s^{-1} (10 s^{-1} at 3 μM MgATP), which is consistent with the results of kinetic studies on full-length S-1 [22]. There was also an indication of a small population of longer-lived attachments (Fig. 2A).

Detached lifetimes also followed an approximately exponential time course (Fig. 2B). Again, the fitted exponents for the two isoenzymes were similar (Fig. 2, legend). The fitted attachment rate constants (governing the detached lifetimes) were approximately one-tenth the attachment rate constants (measured at 3 μM ATP). On a large-population basis one would therefore expect 10% of contact events to occur on top of another one. However, the double events shown by abrupt changes in the displacement of an already stiff portion of the record were rare (Fig. 1), indicating that very few myosin molecules could contact the actin in a given situation.

Acto-myosin attachments took place over the entire range of the thermally generated axial motion of the actin filament (Fig. 1). For both S-1(A1) and S-1(A2), the frequency of contact at different displacement fitted well to a Gaussian distribution (Fig. 3A,B), consistent with the assumption that the probability of attachment depended primarily on the time spent by the filament in a particular longitudinal position. The mean displacement for each isoenzyme was clearly different from the equilibrium position of the unbound filament (Fig. 3), indicating that a working stroke occurred after contact. Nearly all of the contact events fitted to the Gaussian curve, but there was an indication of a small group of events at a large positive bias from the unbound equilibrium position, particularly in S-1(A2) (Fig. 3B). The data from our previous study of full-length papain S-1 [29], obtained under closely similar protocols and on the same apparatus, also gave a good fit to a Gaussian distribution (data not shown).

The bias in the observed distributions caused both the median and the mean of the Gaussian fit to lie below the raw mean (Table 1). We have used the Gaussian fit means to analyse the data rather than the overall means used in previous analyses because we interpreted the bias as due to the separate small population of events described above. On this basis the working strokes of S-1(A1) and S-1(A2) are similar (Table 1). Combining the data, our Gaussian fit estimate of working stroke from chymotryptic S-1 is 3.13 nm (Table 1, column 3). The alternative estimate given by the median of the

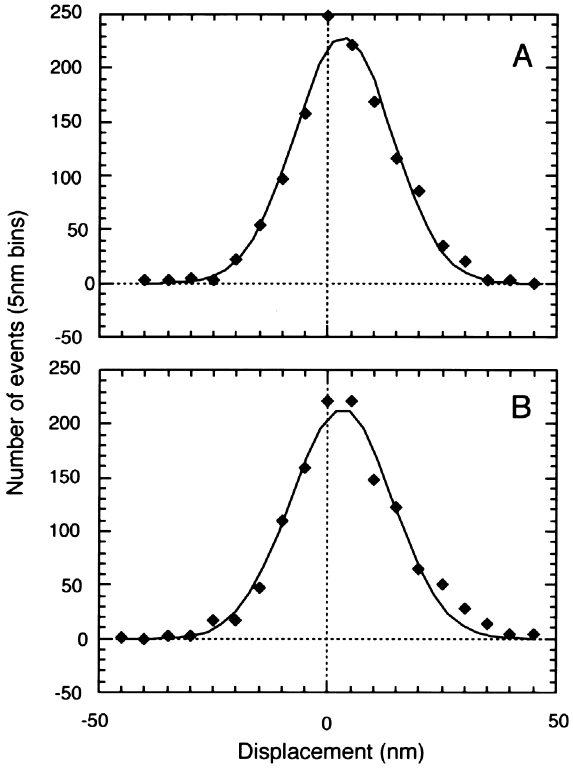

Fig. 3. Frequency of S-1–actin contact relative to the contact's displacement from the equilibrium position of the free filament–bead pair. A: S-1(A1); B: S-1(A2). The lines are single Gaussian fits, performed by fitting the mean, width and height to the 5 nm binned data. Note the bias of the central peak to the right of the mean position of the filament in the absence of contact (the working stroke) and also the small deviation from the fit around +30 nm displacement, which is not matched at −30 nm.

Table 1
Estimates of contact displacement (nm) relative to the equilibrium position of the unbound actin filament

Myosin subfragment	Estimate of displacement			Number of observations
	Mean	Median	Gaussian mean	
S-1(A1)	3.63	3.08	3.15	1321
S-1(A2)	4.00	3.54	3.10	1297
Chymo S-1[a]	3.81	3.30	3.13	2618
Papain S-1[b]	4.73	4.64	4.63	(502)

[a]Combined S-1(A1) and S-1(A2) data.
[b]Analysed from data of [29].

data is 3.30 nm (Table 1, column 2). These two values are, respectively, 68% and 71% of the working stroke obtained from papain S-1 (Table 1). If we ignore the bias and compare the overall means the fraction rises to 80% (Table 1, column 1).

4. Discussion

Single-molecule experiments show that actin and myosin can interact to produce force and displacement [15,17,21,29] which suggests the direct coupling of ATP hydrolysis to a working stroke. Ultrastructural studies of the myosin head have indicated a detailed coupling mechanism [23]. Direct coupling is widely accepted as a working hypothesis, although there is some evidence against it [18,24].

A myosin working stroke could arise in one of two ways, both of which have been considered in the past. The first is a rotation of the entire head about its contact with actin (actin-MD bend [25]), consequent on strengthening of the initial weak bond between the two proteins during the contractile cycle [26]; a similar concept has been considered for kinesin [23]. The second is a rotation of the light chain binding domain about a point close to the distal end of the motor domain (MD-LCD bend) consequent on changes at the enzymatic site during the cycle [1,27]. In both cases, the LCD is considered to act as a rigid lever arm at low load. Shortening it should therefore reduce the unloaded movement produced in proportion to its length from the fulcrum. Removal of the regulatory light chain binding sequence of vertebrate skeletal myosin destabilises the heavy chain α-helix back to the binding of the essential light chain, and hence should shorten the lever arm by approx 3.5 nm [1,8]. This reduces the lever arm to 56% of its length if the bend is at the MD-LCD fulcrum but only to 77% if it is at the actin-MD junction (a loss of 3.5 nm in, respectively, an 8 or 15 nm rotating object; the length estimates used were derived from [1]).

The working stroke of the intact vertebrate skeletal myosin II head, binding both essential and regulatory light chains, has been measured several times under conditions of random surface orientation of the myosin. Early optical trap work on S-1 gave strokes in the range 4–6 nm [21]. Two later studies on heavy meromyosin gave strokes of 5 nm [15,16] and full-length single-headed myosin gave 6 nm [17]. Single-headed myosin assembled into filaments also gave 4–6 nm when aligned 20–40° away from the actin axis, but much more when aligned close to parallel [28]. We have used the data from [29] for comparison with our present data, because they were obtained in the same apparatus and with closely similar protocols. According to our analysis (see Section 3 for details) the chymotryptic S-1 gave 68% of the working stroke of the papain S-1, i.e. approximately halfway between the predictions of the two mechanisms, as if both were in operation.

Such a two-step mechanism has some evidence to support it. In two cases, slow myosins have been shown to produce double working strokes [29,30]; the relatively fast skeletal muscle myosin II used here may therefore be concealing a double event within the limited time resolution of the apparatus. Furthermore, observation of attached myosin heads in isometrically contracting insect flight muscle has shown two classes of distortion: in anti-rigor attachments the entire head rotates about the actin, while in rigor-directed ones the MD-LCD bend changes [3]. Applying such a model to the present data gave a fit to a nearly equal contribution of the two proposed sequential processes (Fig. 4).

Previous workers have obtained data more consistent with the MD-LCD bend hypothesis. Waller et al. [9] found that chymotryptic S-1 supported only half the gliding speed of actin in the in vitro motility assay, and Uyeda et al. [8] found that the *Dictyostelium* constructs with one light chain binding site moved actin at 60% of the speed of ones with two binding sites. More critically, both sets of workers found that motor domain without a light chain binding site moved actin very slowly. Recent data on *Dictyostelium* constructs in the optical trap also support the MD-LCD bend hypothesis [14]. However, other workers have found less effect of LCD length on velocity than would be expected with an MD-LCD bend [7,13].

Two recent developments raise hope that the question may be resolved in other classes of myosin. *Toxoplasma* myosin XIV, which intrinsically lacks an LCD [31], is a priori the most likely myosin class to use an actin-MD rotation, and

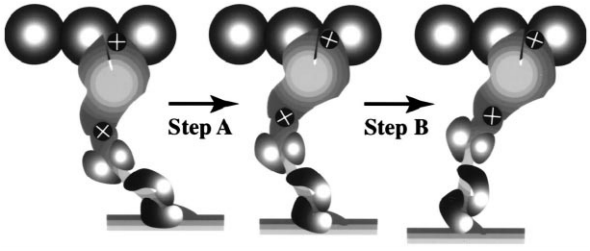

Fig. 4. Model of proposed sequential steps in the working stroke from S-1. Trapped actin above, nitrocellulose-coated surface below; substrate adherence of the myosin heavy chain is assumed to occur close to the C-termination of the light chain binding region. The crosses mark the proposed fulcrums. Step A: actin-MD bend (upper fulcrum); step B: MD-LCD bend (lower fulcrum). Both motions are exaggerated in the figure for clarity. The model fits to the present data when papain S-1 gives 2.6 nm of step A and 2.0 nm of step B, assuming the RLC binding region measures 3.5 nm, the essential light chain (ELC) binding region plus converter region 4.5 nm, and the distance from the MD-LCD fulcrum to the actin-MD fulcrum is 7.0 nm.

might produce a sufficiently large stroke to be incompatible with an MD-LCD bend. The temporal separation of two working strokes in myosins I and V [29,30] also provides a possible means of separating components due to the two mechanisms, since on enzymological grounds [26] the actin-MD rotation should precede the MD-LCD bend.

References

[1] Houdusse, A., Kalbokis, V.N., Himmel, D., Szent-Gyorgyi, A.G. and Cohen, C. (1999) Cell 97, 459–470.
[2] Whittaker, M., Wilson-Kubalek, E.M., Smith, J.E., Faust, L., Milligan, R.A. and Sweeney, H.L. (1995) Nature 378, 748–753.
[3] Taylor, K.A., Schmitz, H., Reedy, M.C., Goldman, Y.E., Franzini-Armstrong, C., Sasaki, H., Tregear, R.T., Poole, K., Lucaveche, C., Edwards, R.J., Chen, L.F., Winkler, H. and Reedy, M.K. (1999) Cell 99, 421–431.
[4] Adhikari, B., Hideg, K. and Fajer, P.G. (1997) Proc. Natl. Acad. Sci. USA 94, 9643–9647.
[5] Sabido-David, C., Hopkins, S.C., Saraswat, L.D., Lowey, S., Goldman, Y.E. and Irving, M. (1998) J. Mol. Biol. 279, 387–402.
[6] Dobbie, I., Linari, M., Piazzesi, G., Reconditi, M., Koubassovaa, N., Ferenczi, M.A., Lombardi, V. and Irving, M. (1998) Nature 396, 383–387.
[7] Itakura, S., Yamakawa, H., Toyoshima, Y.Y., Ishijima, A., Kojima, T., Harada, Y., Wakabayashi, T. and Sutoh, K. (1993) Biochem. Biophys. Res. Commun. 196, 1504–1510.
[8] Uyeda, T.Q.P., Abramson, P.D. and Spudich, J.A. (1996) Proc. Natl. Acad. Sci. USA 93, 4459–4464.
[9] Waller, G.S., Ouyang, G., Swafford, J., Vibert, P. and Lowey, S. (1995) J. Biol. Chem. 270, 15348–15352.
[10] Walker, M., Zhang, X.-Z., Jiang, W., Trinick, J. and White, H.D. (1999) Proc. Natl. Acad. Sci. USA 96, 465–470.
[11] Katayama, E. (1998) J. Mol. Biol. 278, 349–367.
[12] Weiss, S., Herm, A., Geeves, M.A. and Soldati, D. (2000) Biophys. J. 78, 242A.
[13] Anson, M., Geeves, M.A., Kuzawa, S.E. and Manstein, D.J. (1996) EMBO J. 15, 6069–6074.
[14] Ruff, C., Furch, M., Brenner, B., Manstein, D.J. and Myerhofer, E. (1999) J. Muscle Res. Cell Motil. 20, 825–826.
[15] Mehta, A.D., Finer, J.T. and Spudich, J.A. (1997) Proc. Natl. Acad. Sci. USA 94, 7927–7931.
[16] Veigel, C., Bartoo, M.L., White, D.C.S., Sparrow, J.C. and Molloy, J.E. (1998) Biophys. J. 75, 1424.
[17] Tyska, M.J., Dupuis, D.E., Guilford, W.H., Patlak, J.B., Wall, G.S., Trybus, K.M., Warshaw, D.M. and Lowey, S. (1999) Proc. Natl. Acad. Sci. USA 96, 4402–4407.
[18] Kitamura, K., Tokunaga, M., Iwane, A.H. and Yanagida, T. (1999) Nature 397, 129–134.
[19] Margossian, S.S. and Lowey, S. (1982) Methods Enzymol. 85, 55–71.
[20] Taylor, R.S. and Weeds, A.G. (1976) Biochem. J. 159, 301–315.
[21] Molloy, J.E., Burns, J.E., Kendrick-Jones, J., Tregear, R.T. and White, D.C.S. (1995) Nature 378, 209–212.
[22] Lymn, R.W. and Tayor, E.W. (1971) Biochemistry 10, 4617–4624.
[23] Vale, R.D. and Milligan, R.A. (2000) Science 288, 88–95.
[24] Baker, J.E., LaConte, L.E.W., Brust-Mascher, I. and Thomas, D.D. (1999) Biophys. J. 77, 2657–2664.
[25] Huxley, H.E. (1969) Science 164, 1356–1366.
[26] Geeves, M.A., Goody, R.S. and Gutfreund, H. (1984) J. Muscle Res. Cell Motil. 5, 351–361.
[27] Geeves, M.A. and Holmes, K.C. (1999) Annu. Rev. Biochem. 68, 687–728.
[28] Tanaka, H., Ishijima, A., Honda, M., Saito, K. and Yanagida, T. (1998) Biophys. J. 75, 1886–1894.
[29] Veigel, C., Coluccio, L.M., Jontes, J.D., Sparrow, J.C., Milligan, R.A. and Molloy, J.E. (1999) Nature 398, 530–533.
[30] Veigel, C., Wang, F., Bartoo, M.L., Hammer, J., Sellers, J.R. and Molloy, J.E. (1999) J. Muscle Res. Cell Motil. 20, 826.
[31] Heintzelman, M.B. and Schwartzman, J.D. (1997) J. Mol. Biol. 271, 139–146.